

CREEP AND DURABILITY OF POLYMER BASED GEOGRID COMPOSITES

S. Alexeeva^{1*}, A. Mosin¹, I. Viktorova^{1,2*}

¹ Institute of Machines Science of RAS, Malyi Kharitonievsky per., 4, Moscow, RUSSIA, 101990

* Alexeevasofia@yandex.ru

² Clemson University, Department of Mathematical Sciences, Clemson, SC 29634, USA

* Iviktor@clemson.edu

Keywords: creep, durability, polymer materials, strength criterion

Abstract

Geosynthetic materials are polymer-based materials used for reinforcement (i.e., strengthening and arrangement) of soils to enhance their dependability. These materials are widely used in highway engineering; construction of railway embankments and side slopes, both inclined and vertical; and in a number of other applications (filtration, waterproofing and heat insulation of soils, etc.). Depending on the actual applications, these materials can be produced as textiles, various grids, or their combinations, that is, geocomposites. The commonly used load-bearing elements are polymeric materials: PP, polyester, PETP, PE, glass, aramid, shockproof PS, and rigid PVC; the covering materials are usually PVC, PE, or bitumen. Hereditary type model with due account of temperature and moisture effects is developed and presented together with experimental data.

The objective is the mathematical model development for the description of viscous effects and irreversible damage accumulation and for the durability prediction of the viscous materials, such as polymer composites and geogrids.

The analysis is based on Volterra's II-type integral equations or heredity principle. The most general nonlinear equation introduced by Volterra [1] represents an infinite series of the multiple integrals (1):

$$E\varepsilon = \sigma + \int_{-\infty}^t K_1(t-\tau)\sigma(\tau)d\tau + \int_{-\infty}^t \int_{-\infty}^t K_2(t-\tau)\sigma(\tau_1)\sigma(\tau_2)d\tau_1d\tau_2 + \\ + \int_{-\infty}^t \int_{-\infty}^t \int_{-\infty}^t K_3(t-\tau)\sigma(\tau_1)\sigma(\tau_2)\sigma(\tau_3)d\tau_1d\tau_2d\tau_3 + \dots \quad (1)$$

As a result the constitutive equations are constructed with two or three parametric kernels. Let us consider below nonlinear Rabotnov equation, which was suggested in 1948 and widely practiced since [2]

$$\varphi(\varepsilon) = \sigma + \int_0^t K(t-\tau)\sigma(\tau)d\tau. \quad (2)$$

The left-hand side of the equation contains the nonlinear function $\varphi(\varepsilon)$, named the “instantaneous” deformation curve.

Many authors use a kernel in the form of the exponential function $e^{-\beta(t-\tau)}$, which is convenient for the calculations. Its shortcoming is the fact that for short times of loading the calculated results do not correspond to experiments. However, the long term extrapolation can be satisfactory. Attempts to combine the properties of exponent and weak singularity lead to the construction of many kernels: Abel, Bronsky, Slonimsky, Rzhantsyn, Koltunov etc. [3].

The next important question in investigation of polymers and composites with viscous properties is temperature and moisture factors. Principle of joint influence of temperature and humidity is introduced by

$$\varphi(\varepsilon) = \sigma + \int_0^t K(t-\tau) f_1(T) f_2(W) \sigma(\tau) d\tau . \quad (3)$$

It is shown that the function of temperature influence can be chosen as $f_1(T) = T^\gamma$, where T – the temperature measured in Kelvin scale [4]. For the convenience of calculations it can be taken as (4):

$$f_1(T) = \left(\frac{273 + T^{\circ}C}{273} \right)^\gamma . \quad (4)$$

Influence of moisture can be introduced by the same manner [5] by some function $f_2(W)$ under the integral, where W is determined in per cents from weight increasing at moisture-saturation (5):

$$f_2(W) = \left(\frac{W_0 + W\%}{W_0} \right)^\beta . \quad (5)$$

Experimental data allow to justify such approach. It occurs that at increasing of moisture-saturation the effect of creep becomes more pronounced and strain-stress diagrams have the tendency to slip down more and more. On the other hand viscous effects are considerably weaker at drying of a material. The form of the moisture influence function might be the same as the temperature function. Experiments on moisture influence are rather labor-intensive and demand carefully fulfilled measurements with special equipment, so their number in literature is not substantial.

Figures 1 and 2 show examples of temperature and moisture influence on polyoximethylene (POM) and results of calculations with the constitutive equation (3).

Geosynthetic materials are polymeric materials used for reinforcement (i.e., strengthening and arrangement) of soils to enhance their dependability. Depending on the actual applications, these materials can be produced as textiles, various grids, or their combinations, that is, geocomposites. The commonly used load-bearing elements are polymeric materials: PP, polyester, PETP, PE, glass, aramid, shockproof PS, and rigid PVC; the covering materials are usually PVC, PE, or bitumen.

Since objects produced using geosynthetic materials are intended for long-term use (over decades), the primary tasks consist in describing their mechanical characteristics and estimating the level of deformations that would not cause failure of the material during its service life.

It is impossible to perform experiments covering the entire duration of the actual long-term use. At the same time, the existing methods of predicting the behavior of materials (using the techniques of temperature–time analogy and step isotherms) require experiments at elevated temperatures and do not provide highly accurate predictions.

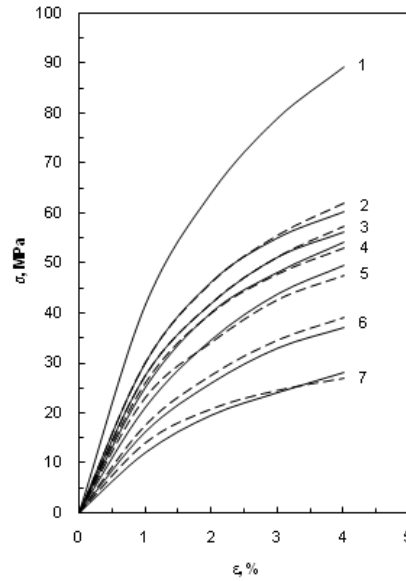


Figure 1. Stress-strain curves of POM for various rates of strain, temperatures and moisture levels:

- 1 - $\varphi(\epsilon)$; 2 - $\dot{\epsilon} = 2 \cdot 10^{-3}$ 1/s, $T = 20^\circ\text{C}$, $W = 0$; 3 - $\dot{\epsilon} = 4 \cdot 10^{-5}$ 1/s, $T = 20^\circ\text{C}$, $W = 0$;
 4 - $\dot{\epsilon} = 2 \cdot 10^{-3}$ 1/s, $T = 20^\circ\text{C}$, $W = 0.45\%$; 5 - $\dot{\epsilon} = 2 \cdot 10^{-3}$ 1/s, $T = 20^\circ\text{C}$, $W = 0.93\%$;
 6 - $\dot{\epsilon} = 2 \cdot 10^{-3}$ 1/s, $T = 60^\circ\text{C}$, $W = 0$; 7 - $\dot{\epsilon} = 2 \cdot 10^{-3}$ 1/s, $T = 80^\circ\text{C}$, $W = 0$.
 ——— experimental and - - - - - calculated results.

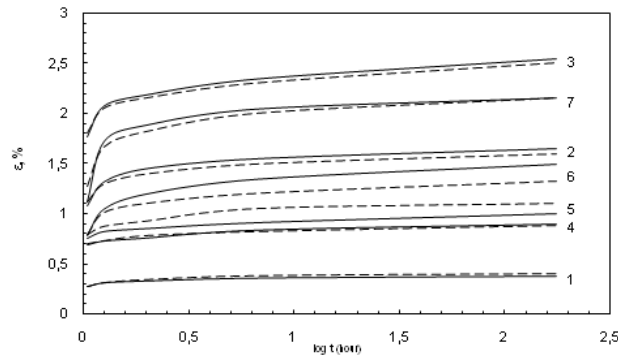


Figure 2. Creep curves of POM at various temperatures, stress and moisture levels:

- 1 - $\sigma = 10$ MPa, $T = 20^\circ\text{C}$, $W = 0$; 2 - $\sigma = 30$ MPa, $T = 20^\circ\text{C}$, $W = 0$;
 3 - $\sigma = 40$ MPa, $T = 20^\circ\text{C}$, $W = 0$; 4 - $\sigma = 20$ MPa, $T = 20^\circ\text{C}$, $W = 0.45\%$;
 5 - $\sigma = 20$ MPa, $T = 20^\circ\text{C}$, $W = 0.15\%$; 6 - $\sigma = 20$ MPa, $T = 60^\circ\text{C}$, $W = 0$;
 7 - $\sigma = 20$ MPa, $T = 80^\circ\text{C}$, $W = 0$. ——— experimental and - - - - - calculated results.

Since geosynthetic materials are made with different polymers, the common feature of both separate elements and large fragments of these materials is their viscoelastic behavior.

The approach proposed in this study makes it possible to predict the behavior of geosynthetic materials during long-term loading using the data of short-term creep experiments. This approach is based on a hereditary-type mathematical model [1,6]. As the underlying relationship, we take a nonlinear hereditary-type integral equation (2).

One of the best known kernels is the Abel kernel (6):

$$K(t-\tau) = \frac{k}{(t-\tau)^\alpha} \quad (6)$$

where $0 < \alpha < 1$. However, this equation has a drawback: at $t \rightarrow \infty$, the strain $\varepsilon \rightarrow \infty$ rather than behaving as an exponent, in contrast to the experimental data.

The properties of an exponent and weak singularity at zero are united, for example, in the Slonimsky kernel [7], which has the form (7):

$$K(t-\tau) = \frac{\gamma \lambda \alpha e^{-\gamma(t-\tau)^\alpha}}{(t-\tau)^{1-\alpha}} \quad (7)$$

($0 < \alpha < 1$, $0 < \gamma$, $0 < \lambda$). However, the disadvantage of this kernel is the difficulty in finding analytical solutions.

The algorithm of finding the parameters of the model for the Abel and Slonimsky kernels is proposed below. It consists in plotting the creep curves, constructing the isochronous creep curves, and directly calculating the parameters. After the values of the kernel parameters are determined, the long-term creep curve can be modified and possible to find the strain value.

The above algorithm has been implemented in a software tool for computer systems written using object-oriented technologies. The software was based on the platform-independent Java programming language.

Let us consider the algorithmic representation of each prediction step in the computer system in more detail. After a long-term creep experiment, one should plot the creep curves $\varepsilon(t)$ within the time range $0 < t \leq 10^3$ h at various load levels. A series of creep curves at a constant stress graphically represents the functional dependence $\varepsilon(\sigma, t)$ plotted in ε and t coordinates for the various σ values.

In most cases, to determine the parameters of the kernel of the integral equation, one should additionally replot the creep curves in the form of isochronous curves. To plot the isochronous curve corresponding to the moment $t = t^*$, one has to obtain a set of points in σ and ε coordinates. Thus, the number of points needed to construct the isochronous curve is just the same as the number of load levels selected for the experiment. The functional description of the isochronous curve is achieved by least-squares interpolation using a power function of the form $\sigma = a\varepsilon^n$.

Let us consider the sets of equations that must be solved to find the values of kernel parameters.

If the Abel kernel is selected, one can integrate the equation (8):

$$\varphi(\varepsilon) = \sigma + \int_0^t \frac{k}{(t-\tau)^\alpha} \sigma d\tau \quad (8)$$

and arrive at the relationship (9):

$$\varphi(\varepsilon) = \sigma(1 + \xi^{1-\alpha}), \quad (9)$$

where $\xi = \frac{k}{1-\alpha}$. Further, for the certain fixed strain value $\varepsilon = \varepsilon^*$, using the constructed isochronous curves, the following set of equations (10) should be solved:

$$\begin{cases} \varphi(\varepsilon^*) = \sigma_1 (1 + \xi t_1^{1-\alpha}) \\ \varphi(\varepsilon^*) = \sigma_2 (1 + \xi t_2^{1-\alpha}) \\ \varphi(\varepsilon^*) = \sigma_3 (1 + \xi t_3^{1-\alpha}) \end{cases} \quad (10)$$

Excluding $\varphi(\varepsilon^*)$ from the resultant set of equations, we obtain the value of

$$\xi = \left(\frac{\sigma_2 t_2^{1-\alpha} - \sigma_1 t_1^{1-\alpha}}{\sigma_1 - \sigma_2} \right)^{-1},$$

where parameter α is found by solving the transcendental equation (11) with respect to α by the dichotomy method on the interval $[0,1]$:

$$\sigma_1(\sigma_3 - \sigma_2)t_1^{1-\alpha} + \sigma_2(\sigma_1 - \sigma_3)t_2^{1-\alpha} + \sigma_3(\sigma_2 - \sigma_1)t_3^{1-\alpha} = 0 \quad (11)$$

After determining the kernel parameters, one can construct the curve of instantaneous deformation $\varphi(\varepsilon)$ and calculate the creep curves for an arbitrary duration of loading.

The parameters of the Slonimsky kernel can be found by a similar method.

The results calculated on the basis of the short-term creep experimental data for the Fortrac-type geogrid made of PETP are given below [8]. The samples of Fortrac-type PETP geogrids were tested under the following regimes: a woven type of the geosynthetic material, a sample width of 3 mm, a sample length of 1000 mm, and a tensile strength of 49 kN/m. The experimental data is shown in Figure 3.

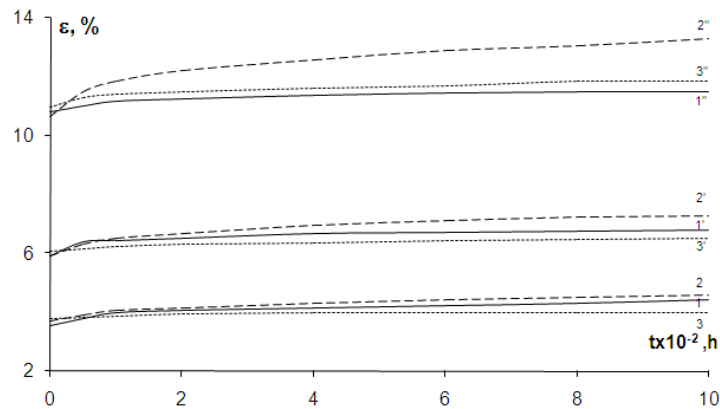


Figure 3. Creep curves for the Fortrac-type geogrid at a load level of (1-3) 5, (1'-3') 10, and (1''-3'') 15 MPa: (1,1',1'') – experimental curves, (2,2',2'') and (3,3',3'') – creep curves plotted using the Abel and Slonimsky kernels, respectively.

According to the first portion of unsteady creep (10 h), the parameters of both kernels were calculated. Further, the kernels with the resultant parameter values were used to perform predictions for the times that were two orders of magnitude larger than the initial times (1000 h). The predicted results were compared with the experimental data.

The use of the Abel kernel yields strain values that are much higher than the experimental ones. The Slonimsky kernel contains a multiplier that ensures an exponential change in strains over time and also provides a good description of the steady-creep portion. The diagram in Figure 3 shows the experimental creep curves and the calculated curves plotted with the use

of the Abel and Slonimsky kernels at various load levels. The parameters of the kernels were calculated at a fixed strain value: $\varepsilon^* = 4\%$. The parameter values turned out to be $\alpha = 0.756$ and $\xi = 0.04$ for the Abel kernel and $\alpha = 0.747$, $\gamma = 0.026$, and $\lambda = 0.578$ for the Slonimsky kernel.

Our calculations and the comparison of predictions with the experimental data showed that the above approach can be used for determining the parameters of various kernels and for predicting the creep of materials during long-term loading. In this case, the Abel kernel gives a more precise description of the creep of the selected experimental material at the initial stage of unsteady creep, whereas the advantage of the Slonimsky kernel is sufficiently accurate description of the material deformation within the steady creep.

The long-term creep and durability analysis [9], based on short-term standard quasistatic and 1000 hours creep experimental data at room temperature had been used to model the mechanical response of polymer-based geogrid “Belgeosot”. The base material for the indicated type of geogrid is polyethylene and this brand is widely used for various industrial applications such as reinforcements of slopes and highway shoulders, in construction, etc.

The dimensions for the tested material specimen were: width – 20 mm; the “working” efficient length – 60 mm. The levels of loading for creep experiments were determined from the quasistatic diagrams as following: 7, 10 and 13 kN/m, which corresponds to 0.2, 0.3 and 0.4 of the ultimate yielding stress level (30 kN/m), respectively. The obtained experimental data is plotted in Figure 4. The creep recovery curves show that for the loading levels of 7 and 10 kN/m the recovery is practically complete with no residual strains observed. However, for the loading level of 13 kN/m, the residual strain is quite significant, which might happen due to the structural changes in the material of geogrid, i.e. due to the continuous damage accumulation and possible elongation of the polymer chains. The analysis of the phenomenon had been based on 1000 hour duration creep experimental data. Thus, the obtained experimental data indicate that the safe loading levels for the analyzed material should not exceed 10 kN/m.

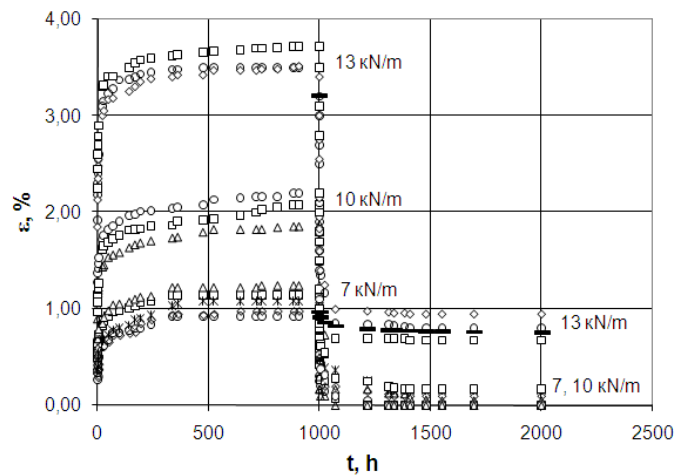


Figure 4. Creep and creep recovery diagrams for the load levels: 7, 10 and 13 kN/m (bold dashed lines – theoretical estimates; geometrical symbols – various experimental data)

The hereditary type constitutive equation used for the numerical analysis of the geogrids under the creep conditions was constructed with two types of integral kernels: two-parametric Abel’s kernel and three-parametric Slonimsky’s kernel [4]. Figure 5 shows the diagrams of experimental and simulated with both kernels creep results for the geogrid, tested for 1000 hours. The reliable parameter estimates can be obtained only from the intervals with the “established” creep, corresponding to 1000 hours testing. The kernels parameters were

determined as following: for Abel’s kernel $\alpha = 0.979$; $k = 0.938$; for Slonimsky’s type - $\alpha = 0.222$; $\gamma = 0.801$; $\lambda = 0.989$.

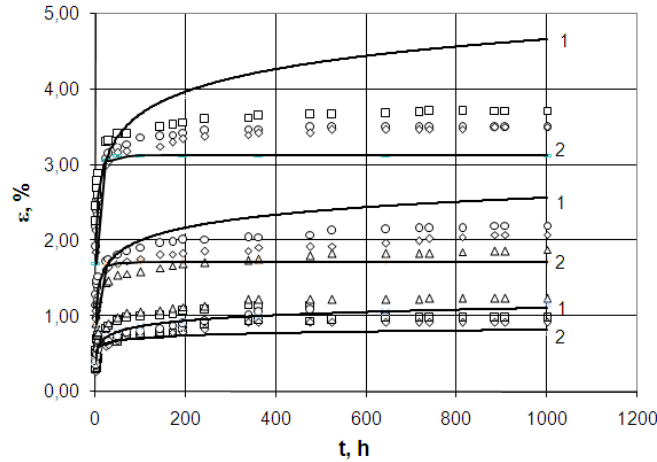


Figure 5. Experimental and theoretical creep diagrams for the loading levels: 7, 10 and 13 kN/m (1 and 2 – the simulated creep diagrams with Abel’s and Slonimsky’s kernels, respectively. The parameters of both kernels were determined from 25 hours creep data)

The instantaneous stress-strain diagrams have been approximated by the power regression and for the case of the Abel’s kernel is defined as: $\varphi(\varepsilon) = 13.9\varepsilon^{0.53}$.

Figure 6 illustrates the simulated model predictions for twenty years ($1.7 \cdot 10^5$ h) of future material use. The plotted theoretical long-term creep curves show the maximum difference (7.5%) in predicted results for the two kernel types at the loading level $F = 13$ kN/m. Therefore, Abel’s kernel had been chosen for further analysis as the most efficient and simple to define.

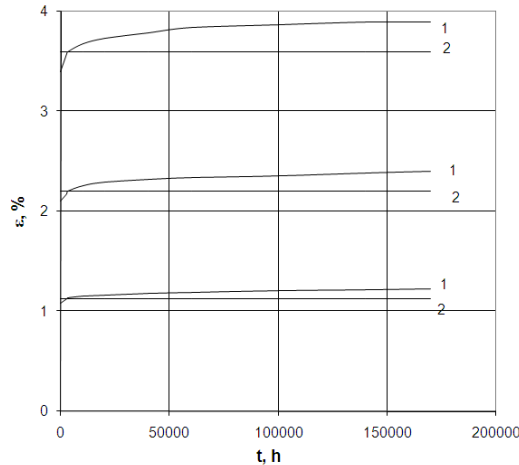


Figure 6. Long-term experimental and theoretical creep diagrams for the loading levels: 7, 10 and 13 kN/m (1 and 2 – the simulated creep diagrams with Abel’s and Slonimsky’s kernels, respectively. The parameters of both kernels were determined from 1000 hours creep data)

Durability model equation has been developed on the basis of damage accumulation analysis

$$\varphi(\varepsilon) = \sigma + \int_0^t L(t - \xi) \sigma(\xi) d\xi + \int_0^t M(t - \xi) \sigma(\xi) d\xi . \quad (12)$$

Here $L(t - \xi)$ is a kernel, which describes reversible viscous deformation, $M(t - \xi)$ describes irreversible damage accumulation process leading to failure.

Detachment of these two kernels during the active loading process is impossible, but can be done if data on failure or unloading processes are available. For description of unloading process from (12) the next equations (13) can be used:

$$\begin{aligned}\varphi(\varepsilon) &= \sigma + \int_0^t L(t-\xi)\sigma(\xi)d\xi + \int_0^t M(t-\xi)\sigma(\xi)d\xi, \quad 0 < \xi < t_* \\ \varphi(\varepsilon) &= \sigma + \int_0^t L(t-\xi)\sigma(\xi)d\xi + \int_0^{t_*} M(t_*-\xi)\sigma(\xi)d\xi, \quad t_* < \xi.\end{aligned}\quad (13)$$

Here t_* is the moment of unloading start.

In the case when material does not possess the viscous characteristics the constitutive equation (14) contains only one kernel, which describes the damage accumulation process:

$$\varphi(\varepsilon) = \sigma + \int_0^t M(t-\xi)\sigma(\xi)d\xi \quad (14)$$

Analysis of equation (14) allows to construct a strength criterion (15):

$$\sigma_0^* = \sigma + \int_0^t M(t-\xi)\sigma(\xi)d\xi \quad (15)$$

Here σ_0^* is maximum point of the instantaneous deformation curve.

The following conclusions are made:

- a) the dependence of strength on the rate of loading – the higher is the rate of loading, the greater is the strength value. This fact can be explained by lower damages in material structure at higher rates;
- b) the dependence of deformation on the rate of loading – the lower the rate of loading, the larger is the value of deformation that corresponds to the moment of loading.

References

- [1] Volterra V. *Theory of functional and of integral and integro-differential equations*. New York: Dover Publ., Inc. (1959).
- [2] Rabotnov Yu.N. *Creep problems in structural members*. Amsterdam-London: North-Holland Publ. Co. (1969).
- [3] Goldman A.Ya. *Strength of the structural members polymers*. Leningrad (1979).
- [4] Suvorova J.V. Temperature account in the hereditary theory of elastic-plastic media. *Problems in strength* (1977).
- [5] Alexeeva S.I. Model of nonlinear hereditary media with temperature and moisture effects. *Doklady Akademii nauk* (2001).
- [6] Volterra V. *Lecons sur la theorie mathematique de la lute pour la vie*. Ganthier-Villars, Paris (1931).
- [7] Slonimsky G.L. On the Deformation Law for Highly Elastic Polymers. *Doklady Akademii nauk SSSR* (1961).
- [8] Suvorova Yu.V., Alekseeva S.I., Kupriyanov D.Yu. Simulation of Long-Term Creep of Fortrac-Type Geogrids Based on Poly(ethylene terephthalate). *Polymer Science* (2005).
- [9] Aschpiz E.S., Suvorova J.V., Alekseeva S.I., Kupriyanov D.Yu., Tatous N.A. Long-Term Creep Modeling for Geogrids. *Zavodskaya Laboratoria. Diagnostika Materialov* (2006).